Structural relations between lyotropic phases in the vicinity of the nematic phases

Y. Hendrikx, J. Charvolin

J. Physique **42** (1981) 1427-1440 OCTOBRE **1981**, PAGE 1427

Classification
Physics Abstracts
61.30E — 82.70

Structural relations between lyotropic phases in the vicinity of the nematic phases (*)

Y. Hendrikx and J. Charvolin

Laboratoire de Physique des Solides (**), Bâtiment 510, Université Paris-Sud, 91405 Orsay, France

(*Reçu le 19 février 1981, accepté le 5 juin 1981*)

Résumé. — Les phases « nématiques lyotropes » sont des fluides anisotropes, solutions aqueuses d'agrégats anisotropes finis de molécules amphiphiles. Leur comportement nématique (écoulement, orientation en champ magnétique) résulte des corrélations orientationnelles entre ces agrégats. Ces phases représentent dans le domaine des cristaux liquides lyotropes des états d'ordre intermédiaire entre les phases ordonnées, lamellaire, hexagonale ou cubique et les phases micellaires totalement désordonnées.
Dans ce manuscrit on tente de dégager les conditions qui sont à l'origine de l'apparition des phases nématiques dans le système décyl sulfate de sodium/1-décanol/eau. A cette fin on explore le diagramme de phase au voisinage de celles-ci. Les différentes phases sont identifiées par leurs textures et leurs structures sont déterminées par diffraction de rayons X aux petits angles. A partir de ces études on peut dégager les effets induits par la variation en concentration de deux paramètres importants, à savoir le décanol et l'eau. Quand la concentration en décanol augmente on observe que la courbure interfaciale des agrégats amphiphiles décroît (une phase hexagonale dont les agrégats sont des cylindres infinis est progressivement substituée par une phase lamellaire ; les phases intermédiaires sont soit des phases dont les agrégats sont des rubans infinis, soit dans certains cas des phases nématiques). Par ailleurs lorsque la teneur en eau augmente, la courbure interfaciale des agrégats amphiphiles croît et les agrégats se désordonnent progressivement (une phase lamellaire est dans un premier temps substituée par une phase dont les agrégats sont des rubans infinis, ensuite une phase « nématique » dont les agrégats sont des sphéroïdes prolats apparaît, puis une phase « nématique » dont les agrégats sont des sphéroïdes oblats pour atteindre enfin une phase micellaire totalement désordonnée). Le décanol et l'eau déterminent donc la forme, les dimensions et l'organisation des agrégats de manières antagonistes : on peut considérer que les phases « nématiques lyotropes », localisées dans un domaine très étroit du diagramme de phase, résultent d'un compromis entre les actions conjuguées de ces deux paramètres.

Abstract. — « Nematic lyotropic » phases are anisotropic fluids made of aggregates of amphiphilic molecules dispersed in water. Their nematic behaviour (flow, orientation in a magnetic field) is related to the orientational correlations between the aggregates which are anisotropic particles of finite dimensions. Therefore they are examples in the field of lyotropic liquid crystals of intermediate states of organization between the well known ordered lamellar, hexagonal or cubic phases and the totally disordered micellar phases.
This paper presents an attempt to determine the conditions governing the occurrence of nematic phases in the system sodium decyl sulfate/1-decanol/water. For this purpose the ternary phase diagram is investigated in the vicinity of the nematic phases, first the various lyotropic phases are recognized according to their textures, then their structures are determined through small angle X-ray scattering. From these observations the effects induced by changing the two most obvious parameters, the concentrations of decanol and water, are as follows. When the phase diagram is crossed towards increasing decanol concentration the curvature of the amphiphile-water interface decreases (an hexagonal phase made of infinite cylinders is replaced by a lamellar phase, intermediate phases made of infinite ribbons and in some cases « nematic » phases may appear in between). On the other hand, when the water content is increased, the curvature of the amphiphile-water interface increases and the stacking of the aggregates becomes more disordered (a lamellar phase is first replaced by a phase made of infinite ribbons, thereafter by a « nematic » phase made of prolate spheroids, then by a « nematic » phase made of oblate spheroids or discs, and finally by a fully disordered micellar phase). Therefore decanol and water control the shapes, sizes and packing of the aggregates along antagonistic ways and the « nematic » phases, which occupy a very limited area in the phase diagram may be considered as resulting from the delicate interplay of these two parameters.

(*) Part of this work was presented at the Conference on « Liquid Crystals of One- and Two-Dimensional Order » (Garmisch-Partenkirchen 1980).

(**) Laboratoire associé au C.N.R.S. (L.A. nº 2).

1. **Introduction.** — The polymorphism of lyotropic mesophases illustrates the wide range of states of organization for amphiphilic molecules in water. The typical ordered liquid crystalline phases of amphiphile-water systems are made of infinite aggregates of amphiphilic molecules which are themselves arranged with some long range translational order (periodicity of the density in one, two or three dimensions). On the other hand, the totally disordered micellar phases are made of finite spherical or ellipsoidal aggregates. In 1967, Lawson and Flautt [1] made some new phases by adding small amounts of a long chain alcohol (1-decanol) and salt (sodium sulfate) to a classical water-amphiphile system (sodium decyl sulfate or SdS [2]). These phases appeared as anisotropic fluids whose properties (texture and spontaneous orientation in a magnetic field) are similar to those of thermotropic nematics. For this reason they were called « lyotropic nematics ». Since 1967, many other systems, forming lyotropic nematic phases, have been investigated [3-7]. Up to now they fall into two classes according to the way they orient in a magnetic field [7]. They are said to be of type I when they have a positive anisotropy of magnetic susceptibility $\Delta\chi$, their director aligns along the field. They are said to be of type II when $\Delta\chi < 0$, their director orients perpendicular to the field.

The structure of these phases has been studied recently through small angle X-ray scattering in the system SdS-decanol-water [8]. It has been shown that in these phases the molecules are assembled in aggregates, as in any other lyotropic liquid crystal, but which are arranged with orientational order without translational order. The type I phase ($\Delta\chi > 0$) was shown to contain elongated aggregates (prolate spheroids) and following [9] we propose to call it « calamitic » (from $\chi\alpha\lambda\alpha\mu o\sigma$: reed). The type II phase ($\Delta\chi < 0$) was shown to be made of flat particles (oblate spheroids) and we call it « discotic » [9] (from $\delta i\sigma\chi o\xi$: quoit). Therefore we adopt a structural classification for these nematic phases as N_c (calamitic) or N_d (discotic) whereas the first one, as type I or type II was based on magnetic properties [10].

At this stage, in order to define the aim of our work, it is useful to compare these lyotropic nematic phases and the classical lyotropic phases. For this we shall consider the ternary SdS-decanol-water phase diagram as it can be extrapolated from existing data about sodium dodecyl sulfate-decanol-water and sodium octyl sulfate-decanol-water phase diagrams [11]. The approximate location of the nematic phases relative to other known phases is shown in figure 1. The small nematic domain is surrounded by three domains, lamellar hexagonal and micellar, which have been the subject of many structural investigations in various systems [11-17]. In the lamellar and hexagonal domains the amphiphilic aggregates are infinite lamellae or cylinders, periodically packed with long range translational order along one or two dimensions;

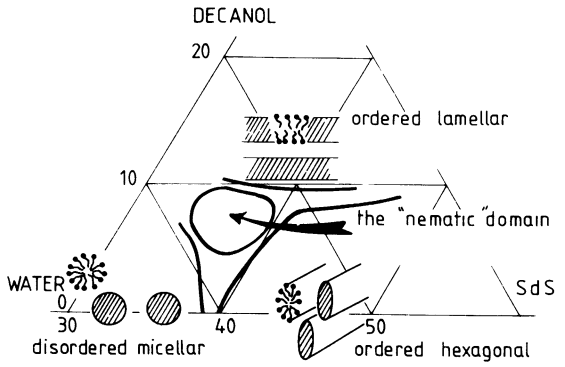

Fig. 1. — Hypothetical SdS-decanol-water phase diagram in the vicinity of the nematic domain extrapolated from existing data on closely related systems (9). (Concentrations in weight per cent.)

macroscopically the phases appear rather viscous and optically anisotropic. In the micellar domain the aggregates are finite spheres or ellipsoids without any long range ordering; the phase is fluid and isotropic. It is interesting to remark here that the properties of fluidity and anisotropy are associated together only in the nematic domain. The orientationally ordered nematic phases may therefore be considered as intermediate states of order between the translationally ordered lamellar and hexagonal phases and the totally disordered micellar one. In this paper, we try to determine the conditions governing the occurrence of the nematic states by studying their structural relations with the neighbouring ordered or disordered phases. We have therefore investigated the SdS-decanol-water phase diagram by mean of optical observation in order to classify the phases according to their texture, then, within each phase, the structures of a few samples have been determined by X-ray diffraction.

2. **Samples.** — Sodium decyl sulfate was either prepared in the laboratory [18] or was of commercial origin (Merck p.p.a. 99 %), 1-decanol was commercial (Fluka p.p.a. > 99 %); (samples with identical composition, prepared either with SdS synthesized in the laboratory or with the commercial SdS had the same properties).

The samples were prepared in sealed tubes by weighting of the appropriate quantities of the compounds and homogeneized through ultra-sonication and centrifugation. To get stable samples all glass material must be perfectly clean, without any fatty impurities, furthermore the temperature during the homogeneization has to be maintained below 50 °C in order to prevent the hydrolysis of SdS into decanol [19] which displaces the sample from the nematic domain towards the lamellar one.

3. **Experimental methods.** — 3.1 TEXTURES. — The nature of the samples, ordered lamellar or cylindrical, nematic, disordered micellar, were first identified by

observing their textures in polarized light. The samples were smeared in between glass plates and observed under a polarizing microscope equipped with heating stage and camera (Leitz).

3.2 STRUCTURES. — The structures of the samples were obtained by small angle X-ray diffraction. (We shall use the following notation : $| \mathbf{s} | = \frac{2 \sin \theta}{\lambda}$ where $\mathbf{s}$ is the scattering vector, λ the wave length and 2θ the angle between scattered and incident beams.) Three different set-ups were used according to the nature of the sample.

3.2.1 *Phases with long range translational order.* — In this case the samples are naturally polycrystalline and they were studied with a Guinier's camera for small angle studies of powdered samples [20] ; (monochromatic Co, $K\alpha_1$ radiation, wave length $\lambda = 1{,}788\,9$ Å, linear collimation, diameter of the camera = 125 mm). The samples were in between mica sheets separated by a teflon spacer of thickness 0.7 mm ; the whole cell, whose tighness was ensured by a set of joints and a mechanical clamping, was placed in a thermostated enclosure [21].

This camera has been used very successfully to characterize structures of the lyotropic systems [13]. Its advantage is that a wide range of angles may be investigated with high resolution because the X-ray beam is always focused on the curved photographic film. In the small angle region [$s \sim (40\ \text{Å})^{-1}$] the diffraction pattern corresponds to the long range organization of the amphiphilic aggregates. A set of reflections is observed, whose angles give access to the symmetry and to the parameters of the unit cell. From these, knowing the volume fraction occupied by each compound of the sample, a first approximation of the shape and dimensions of the aggregates can be obtained [16]. (One way to determine the form factor of the aggregate is to compare quantitatively the intensities of the various reflections. This would provide a better description about their shape. This has not been done here. However in one particular case as will be mentioned in paragraph 5.1.2 and discussed in Appendix II, the relative intensities of the reflections were analysed succinctly.) The diffraction in the large angle region [$s = (4.5\ \text{Å})^{-1}$] provides information about the short range organization of the amphiphilic molecules within the aggregates ; in all the cases studied here a diffuse band was observed showing the local disorder of these molecules [13].

3.2.2 *Oriented nematic phases.* — These phases only show a diffuse band in the small angle region, indicating that the aggregates are no longer arranged with long range translational order. This makes it difficult to extract the structure factor from the scattering of a polycrystalline sample. Fortunately these nematic phases can be oriented by a magnetic field ; thus the packing of the aggregates along different directions can be studied, giving access to an estimate of their dimensions through the knowledge of their volume concentration. The geometry of the Guinier camera is not suitable for such experiments. We used a monochromatic Laue camera with point collimation (Cu, $K\alpha_1, \lambda = 1{,}54$ Å) equipped with a movable 12 kG permanent magnet. The resolution of this camera varies with the angle because of the photograph film is planar ; however we have used it only in a limited small angle region where it was focused. The sample were in sealed glass capillaries of diameter 1.5 mm, held perpendicular to the X-ray beam. They were oriented by the magnetic field in the equatorial plane. The director aligns along the field when $\Delta\chi > 0$ and orients perpendicular to the field when $\Delta\chi < 0$. For both samples the diffraction patterns were obtained for two configurations with the X-ray beam either parallel or perpendicular to the director. (To get the X-ray beam parallel to the director the samples were oriented by the magnetic field outside the Laue camera.) In this way two sections of the reciprocal space, parallel and perpendicular to the director respectively, were obtained, giving access to the average symmetry and two dimensions of the diffracting element. The detailed analysis of the diffraction patterns were given elsewhere [8]. From them it appears that the aggregates are either calamitic (here $\Delta\chi > 0$) or discotic (here $\Delta\chi < 0$).

3.2.3 *Disordered micellar phases.* — In this case the absence of any order prevents us from gaining direct access to either the form factor of the aggregates or their distribution. But if the small angle scattering is measured on an absolute scale some parameters may be found out and a systematic structural analysis can be made [21-23]. The absolute measurements were obtained with a spectrometer equipped with a photon counting detector (monochromatic radiation Cu, $K\alpha_1$ wave length $\lambda = 1{,}54$ Å, point collimation). This experimental set-up was described elsewhere [24], we shall just briefly recall its principle. The intensity of the radiation scattered by the solution is collected through a circular slit on a Si-Li detector protected by a beryllium window. The variation of the measuring angle is ensured, for a given average radius of the slit, by varying the sample-detector distance while keeping the incident beam as symmetry axis.

The samples, 1 mm thick, were enclosed in perfectly tight cells similar to the ones described above [§ 3.2.1]. The measured energy $E(s)$ scattered by a sample for an average scattering vector $\mathbf{s}$, within a solid angle $\Delta\Omega$, gives access to the total scattering intensity, $I(s)$, which contains terms coming from the micelles, the SdS monomers, the solvent and the windows of the container. As described in Appendix I, it was possible to estimate the concentration of monomers ; it was found $< 1.8 \times 10^{-2}$ M ; therefore it remains smaller than 10 % of the total SdS concentration even for our most dilute sample ; for this reason its contribution to the total scattering intensity of the sample is negligible. The contribution of the solvent was obtained

from separate spectra measured in the same experimental conditions as for the samples. Finally the contribution of the solvent, and that of the container was eliminated by subtracting the intensity scattered by the solvent from that scattered by the samples in similar containers, as written in (1) :

$$\overset{\text{micelles}}{I(s)} = \frac{\overset{\text{sample}}{E(s)}}{\Delta\Omega\, T^{\text{sample}}} - \frac{\overset{\text{solvent}}{E(s)}}{\Delta\Omega\, T^{\text{solvent}}} = \frac{\overset{\text{micelles}}{E(s)}}{\Delta\Omega} \quad (1)$$

where T^{sample} and T^{solvent} are the transmissions of the sample and the solvent in their containers. The absolute scattering intensity $\overset{\text{m}}{I}(s)$ per unit volume of a sample of thickness e is :

$$\overset{\text{micelles}}{I(s)} = \overset{\text{m}}{I}(s) = \frac{\overset{\text{m}}{E(s)} \times S}{\Delta\Omega \times I_e \times E_0 \times V} = \frac{\overset{\text{m}}{E(s)}}{\Delta\Omega \times I_e \times E_0 \times e} \quad (2)$$

where S is the section of the incident beam, I_e the scattering cross section of one electron [20] and E_0 the energy of the direct incident beam. Later on the normalized intensities

$$I_n(s) = \frac{\overset{\text{m}}{I(s)}}{\overline{\rho}},$$

i.e. the scattering intensities per electron of the sample will be used ; ($\overline{\rho}$ is the mean electron density of the sample). E_0 was determined with a reference sample of water. Indeed, the scattering intensity of water is known to be independent of **s** within the range of our measurements and equal to 6.4 e^-/molec. [25]. Thus,

$$\overset{H_2O}{I(s)} = 6.4\, e^-/\text{molec.} = \frac{\overset{H_2O}{E(s)}}{\Delta\Omega \times I_e \times E_0 \times e \times T^{H_2O} \times N} \quad (3)$$

where $\overset{H_2O}{\frac{E(s)}{\Delta\Omega}}$ is the scattered intensity from which the contribution of the window of the container has been subtracted, T^{H_2O} the transmission of water measured in its container and N the number of water molecules per unit volume. In this way, the absolute scattering intensity $\overset{\text{m}}{I}(s)$ of relation (2) was calculated for each sample for 1.96×10^{-2} Å^{-1} < **s** < 6.77×10^{-2} Å^{-1}.

4. **Phase diagram.** — We have studied the region of the phase diagram shown in figure 1 which surrounds the nematic phases. In this region the concentrations of the samples, expressed in weight per cent vary in the following ranges : H_2O 41.6 to 6.3 % ; SdS 33.5 to 57.4 % ; decanol 0 to 13.4 %. The temperature was 22 °C.

Observations between two crossed polarizer plates of the samples in their preparation tubes permit their coarse classification as mono, bi or triphasic, isotropic or anisotropic.

4.1 ISOTROPIC SAMPLES. — The isotropic samples which have a low water content (close to the nematic domain) exhibit a very interesting behaviour : they appear black between the crossed polarizers when at rest but are illuminated by flashes of light when they are submitted to a shock. This induced birefringency suggests that these samples contain some unoriented anisotropic aggregates which orient under shear ; alternatively, but less likely, the birefringency could be produced by a deformation under shear of isotropic aggregates. Moreover these samples also become anisotropic when they are put in a magnetic field. This behaviour will be explained by the forthcoming structural study.

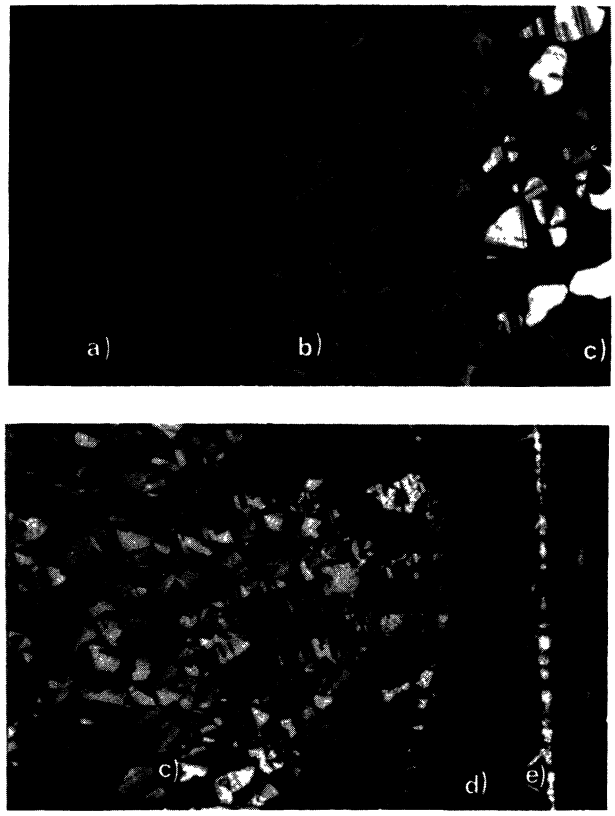

Fig. 2. — Sequence of textures observed from the centre towards the edge of the preparation when a N_d nematic sample smeared in between two glass plates is allowed to dry by its edges (line B in Fig. 3). *a*) N_d nematic phase ; *b*) N_c nematic phase ; *c*) ordered cylindrical phase ; *d*) ordered lamellar phase ; *e*) anhydrous SdS-decanol mixture.

4.2 ANISOTROPIC SAMPLES. — For anisotropic samples the study of their textures under the polarizing microscope provides a way to identify the phases as nematic, lamellar or cylindrical, thus refining the first coarse classification. The textures of these phases are now well known [3, 4, 6, 11, 26] and permit a rapid identification. This is illustrated by the sequence of textures shown on the photograph of figure 2. Here a N_d nematic sample smeared in between two glass plates was allowed to dry by its edges so as to establish a gradient of water concentration from the centre towards the edge of the preparation. As decanol, insoluble in water, is entirely solubilized by SdS it may be assumed that the evaporation of decanol is negligible. Thus the photograph of figure 2 represents the evolution of the sample at constant SdS/decanol ratio, from the N_d nematic on the left towards more concentrated phases on the right (line B drawn on the phase diagram sketched in figure 3 at the end of this paragraph). On the extreme left (a) the stage is totally black, this is the texture of the N_d sample in a homeotropic configuration. Under drying (b) a threaded like texture grows which corresponds to the transition of the sample towards a N_c nematic [27]; both textures of N_d and N_c nematic phases are simultaneously apparent, at this stage demixion probably occurs. Then (c) a fan-like texture develops which is characteristic of two-dimensional packing of infinite cylindrical aggregates [26, 28, 29]. However, this particular texture observed here is remarkable by the highly contrasted areas within the fans. This had not been hitherto observed with classical cylindrical phases of hexagonal symmetry [26]. At this stage this phase can be described as a cylindrical phase but not necessarily with hexagonal symmetry; this point is confirmed and enlightened by the structural study presented in paragraph 5.1.2. In (d) the texture changes again into a black area with white crosses (or four-leaved clovers) typical of a lamellar phase whose layers run in average parallel to the glass plates; the crosses correspond to defects associated with Dupin's cyclides. Finally at the extreme right of the preparation (e) a thin edge of anhydrous SdS-decanol mixture is seen.

A picture of the phase diagram, more accurate than that in figure 1, may now be sketched in figure 3. Several zones are delimited, the limits of which are only approximatively sketched because the transformations from one phase to another have not been approached systematically. The next section will present a determination of the structure of typical samples within each zone of this phase diagram.

5. **Structures.** — 5.1 PHASES WITH LONG RANGE TRANSLATIONAL ORDER. — We shall discuss here the X-ray patterns of three samples with increasing decanol content but almost the same amphiphile water ratio. They are successively (see Fig. 3, line A) : sample α (SdS : 52.5 %, H_2O : 47.5 %, decanol : 0 %), sample β (SdS : 47.2 %, H_2O : 47.6 %, decanol : 5.2 %), sample γ (SdS : 41.9 %, H_2O : 47.3 %, decanol : 10.8 %). In each case the small angle region of the diffraction pattern shows a set of narrow reflections characteristic of an ordered system (Fig. 4). We have indexed these reflections, determined the symmetry of the lattice and characterized the structure of the phases following reference [30]. The equations that define the spacing of the reflections for the different symmetry

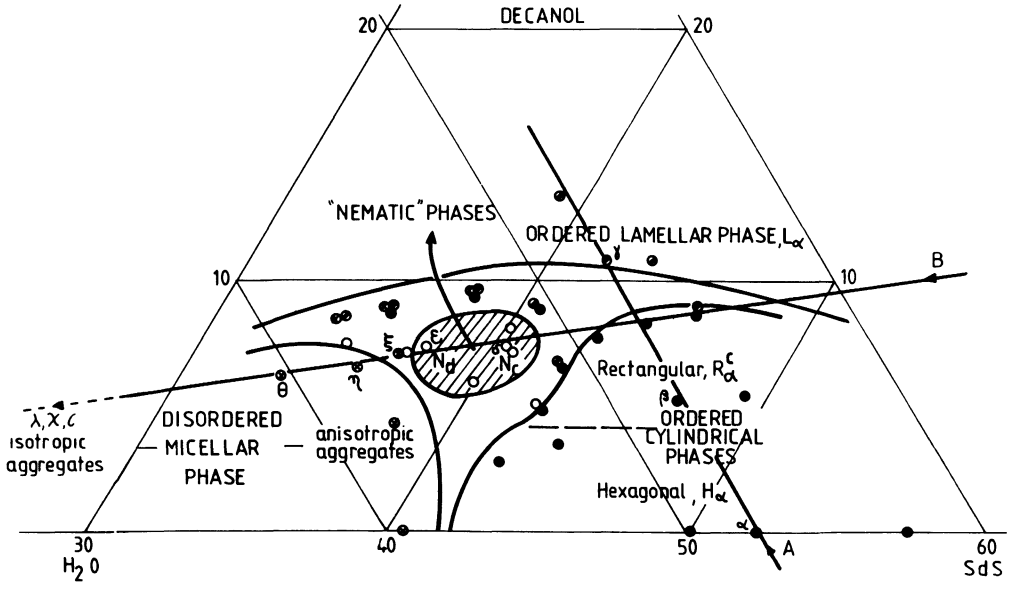

Fig. 3. — Region of the SdS-decanol-water phase diagram where the lyotropic nematic phases and their adjacent phases (ordered lamellar, ordered cylindrical and disordered micellar) are located. (Concentrations in weight per cent.) The limits are only indicative as we have not studied the phase transitions. (● viscous anisotropic phases : ○ fluid and clear anisotropic phases : ⊘ fluid and turbid anisotropic phases ; ⊗ isotropic phases : juxtaposed points indicate polyphasic samples).

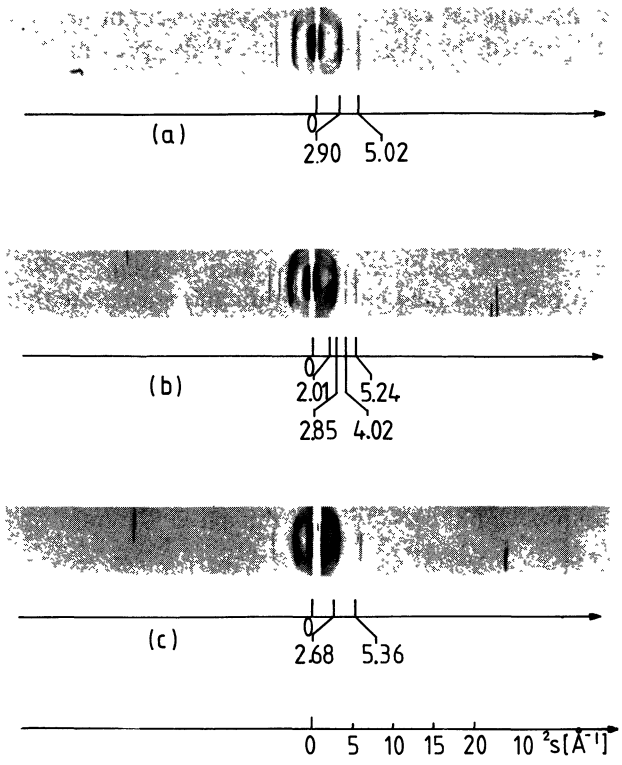

Fig. 4. — Diffraction patterns of phases with long range translational order : *a*) sample α, primitive hexagonal lattice, H_α phase ; *b*) sample β, centred rectangular lattice (space group cmm), R_α^c phase. Indexation of the reflections :

h	k	$10^2\, s\,(Å^{-1})$
0	2	2.01
1	1	2.85
0	4	4.02
2	0	5.24

c) sample γ, lamellar lattice, L_α phase.

systems with periodicities along one or two dimensions are :

— *Periodic in one dimension : lamellar*

$$s_l = l/d\,. \tag{4}$$

— *Periodic in two dimensions*

$$\begin{cases} \text{oblique } s_{hk}^2 = h^2 a^{*2} + k^2 b^{*2} - 2hka^* b^* \sin\gamma \\ \qquad \sigma = (a^* b^* \sin\gamma)^{-1} \end{cases} \tag{5}$$

$$\begin{cases} \text{rectangular } s_{hk}^2 = h^2 a^{*2} + k^2 b^{*2} \\ \text{primitive} \quad \sigma = (a^* b^*)^{-1} \end{cases} \tag{6}$$

$$\begin{cases} \text{rectangular } s_{hk}^2 = h^2 a^{*2} + k^2 b^{*2} \quad (h+k=2n) \\ \text{centred} \quad \sigma = (2\, a^* b^*)^{-1} \end{cases} \tag{7}$$

$$\begin{cases} \text{hexagonal } s_{hk}^2 = a^{*2}(h^2 + k^2 - hk) \\ \text{primitive} \quad \sigma = (2/\sqrt{3})\, a^{*-2} \end{cases} \tag{8}$$

with :

s_{hkl} : reciprocal spacing ($Å^{-1}$) of the reflection of indices h, k and l,

a^*, b^*, γ : dimensions and angle of the reciprocal unit cell,

d : repeat distance of the lamellar phase,

σ : area of the primitive two-dimensional cell.

The symmetry of the lattice is determined by finding out which equation fits the observed spacings. When the symmetry is found, the dimensions of the unit cell can be calculated.

5.1.1 *Sample* α (Fig. 4*a*). — The texture of that sample is that of a phase with infinite cylindrical aggregates ordered with hexagonal symmetry. This is confirmed by the X-ray pattern of figure 4*a* where the spacings of the two diffraction orders are in the ratio $1, \sqrt{3}$; they can be indexed in accordance with equation (8), therefore the lattice is hexagonal primitive and the phase can be denoted H_α (following V. Luzzati's notation). It is reasonable to assume that the symmetry of the structure element is higher than that of the lattice so that we may consider that the sections of the cylinders are circular as shown in figure 5*a*. The lattice parameter, a, which is here also the distance between cylinders, can therefore be calculated, $a = 36.5$ Å. Then knowing the concentrations of amphiphile and water, we can deduce the area S of the normal section of one cylinder, $S = 531$ Å^2, hence the diameter D of the cylinders, $D = 26$ Å and the mean area A occupied by the amphiphile molecule at the amphiphile-water interface, $A = 56$ Å^2 [16].

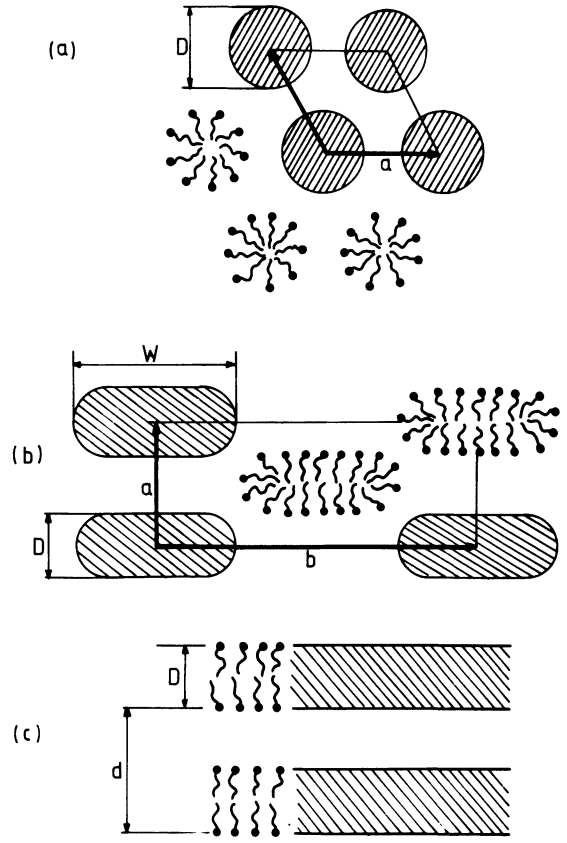

Fig. 5. — Schematic representation of cross sections of the lattices whose diffraction patterns are reproduced in figure 4 and of the cross section of their structure elements. *a*) 2D hexagonal lattice, H_α ; *b*) 2D centred rectangular lattice, R_α^c ; *c*) 1D lamellar lattice, L_α.

5.1.2 *Sample β* (Fig. 4*b*). — This sample also shows a texture corresponding to a periodic assembly of infinite cylinders, i.e. to system with two-dimensional order. However the reflections shown in figure 4*b* cannot be indexed according to the hexagonal primitive lattice, as for sample α, the best fit is obtained assuming a centred rectangular lattice, equation (7). That phase will be noted R_α^c. In this situation the sections of the cylinders can no longer be circular. The rectangular lattice suggests a ribbonlike shape for aggregates; this is supported by an analysis of the relative intensities of the reflections (see Appendix II). A section of the lattice is shown in figure 5*b*. Knowing the lattice parameters, the concentrations of amphiphile molecules and water, we can deduce the area S of the normal section of a ribbon, $S = 934$ Å^2. If we assume that the thickness of the ribbon D is that of the bilayer in the lamellar phase (see sample γ below) i.e. $D = 19$ Å, then the width of the ribbon is $W \sim 49$ Å and the area per amphiphile molecule $A \sim 53$ Å^2. (A similar X-ray pattern has been obtained in one instance where a N_c nematic sample was dried up in the vacuum chamber of the camera : this observation agrees perfectly with the photograph in figure 3*c*.)

5.1.3 *Sample γ* (Fig. 4*c*). — The texture of this sample is that of a lamellar phase. The spacings of the reflections in figure 4*c* are in the ratio 1, 2; they can be indexed in accordance with equation (4). Therefore, the lattice is a lamellar lattice periodic along one dimension as shown in figure 5*c* and the phase will be denoted L_α. The lattice parameter, which is also the distance d between two lamellae is $d = 37.3$ Å. Knowing the concentrations of amphiphile molecules and water we can deduce the thickness D of one soap lamella, $D = 19$ Å, and the mean area A per amphiphile molecule at the interface, $A = 37$ Å^2.

5.2 Ordered nematic phases. — The analysis of our first X-ray diagrams of oriented samples with the Laue Camera have been given elsewhere [8, 31]. We shall just recall here the essential conclusions for two samples (see Fig. 3) δ (SdS : 40.32 %, H_2O : 52.48 %, decanol : 7.2 %) and ε (SdS : 37.50 %, H_2O : 55.06 %, decanol : 7.44 %).

5.2.1 *Sample δ*. — For this type I sample ($\Delta\chi > 0$), the aggregates are elongated cylinders which are nearly parallel to each order at a lateral distance of about 38 Å; their average diameter is about 30 Å, but we have no information about their lengths. This is a N_c phase. On this last point, it is possible to imagine either infinite cylinders (as in the ordered phases) or finite ones; in the latter case, if they are monodisperse they must be longer than 150 Å which is the largest distance accessible with our apparatus; alternatively, the cylinders might well be very polydisperse in their lengths; then the broadening of the X-ray pattern might be such that the length distribution cannot be measured.

5.2.2 *Sample ε*. — For this type II sample ($\Delta\chi < 0$) the aggregates are flattened discs with a thickness of 20 Å and an average diameter of about 60 Å; these discs are nearly parallel to each other at distances of about 37 Å along their axis and 72 Å perpendicular to it. This is a N_d phase.

(The N_d, or type II, phase of the same system has also been studied by L. Q. Amaral *et al.* [32]. These authors also conclude to the existence of lamellar aggregates, but with diameter ten times larger. Also, the lines which we have observed in our scattering experiments are absent from their spectra.)

The values quoted here (§ 5.2.1 and § 5.2.2) refer to a rather limited number of studies. Systematic investigations of the variations of the dimensions of these aggregates with temperature, concentration and the nature of the system are on the way [33].

5.3 Disordered phases. — The structure of the aggregates in the isotropic domain (micellar solution) was investigated for 6 samples with the same SdS/decanol ratio (3.35) and increasing water contents. The normalized intensities $I_n(s)$ are shown in figures 6 and 7. They are smooth curves whose maxima at $s \sim (36$ Å$)^{-1}$ do not vary appreciably with the water content. Most likely this holds to the fact that in those systems, the mean distances between the aggregates are comparable to their dimensions (for the concentrated micellar solutions containing aggregates with diameter ~ 35 Å, the mean distance would be ~ 50 Å). Thus both inter and intra aggregate interferences contribute to the scattered intensities in the vicinity of the peaks shown in figures 6 and 7. This makes it difficult to use the region of the scattering curves corresponding to $s < (36$ Å$)^{-1}$.

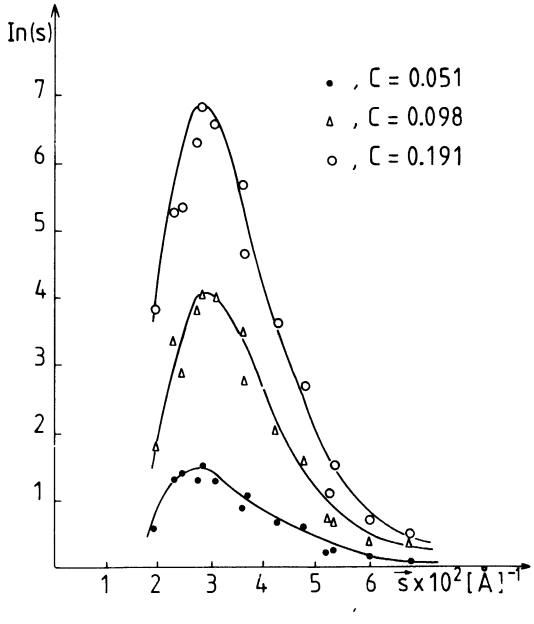

Fig. 6. — Diluted disordered phases. Experimental curves $I_n(s)$ (normalized intensities) for different concentrations. C = amphiphile concentration expressed in grams of solute per gram of solution.

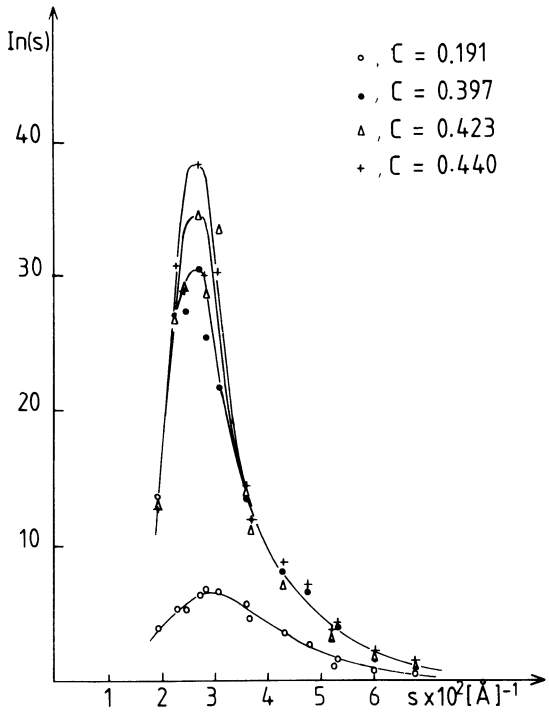

Fig. 7. — Concentrated disordered phases. Experimental curves $I_n(s)$ (normalized intensities) for different concentrations. C = amphiphile concentration expressed in grams of solute per gram of solution.

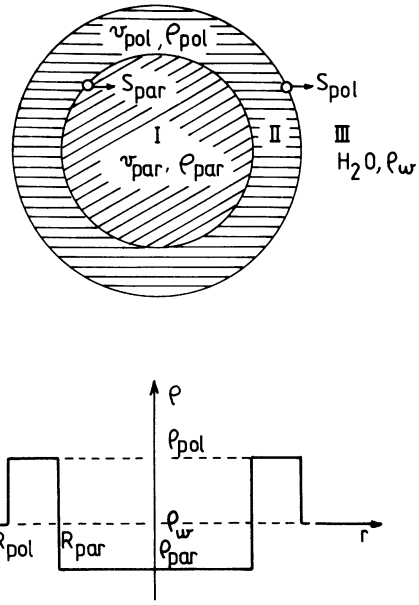

Fig. 8. — Schematic representation of a spherical micelle and of its radial electron density in water. I : Paraffinic region, assumed to be compact without water ; its volume is v_{par} and its electron density $\rho_{par} = 0.272\ e^-/Å^3$; II : Interfacial region containing the polar heads, all their gegenions and water ; its volume is v_{pol} and its electron density ρ_{pol} ; III : Water region, its electron density is $\rho_w = 0.327\ e^-/Å^3$; S_{par} : surface of discontinuity between ρ_{par} and ρ_{pol} ; S_{pol} : surface of discontinuity between ρ_{pol} and ρ_w ; R_{par} : radius of the paraffin core ; R_{pol} : radius of the micelle.

The same problem was met by F. Reiss Husson and V. Luzzati [22, 23] who developed a method using the scattering at larger angles (beyond the interference peaks) to determine the shape of the aggregates ; we shall follow this method here.

The intensity at larger angles ($s > (36\ Å)^{-1}$) is dominated by short range fluctuations of the electronic density within the aggregates. In particular the asymptotic shape of the intensity depends upon the surfaces of discontinuity of this density, as shown by Porod [34].

In order to use Porod's law we consider that this density can have three values as shown in figure 8 : ρ_w in water, ρ_{par} in the paraffinic chains (volume v_{par}), and ρ_{pol} in the interfacial region (volume v_{pol}). The areas of the surfaces of discontinuity separating these three regions are denoted S_{par} (surface of the paraffinic region) and S_{pol} (outer surface of the polar region). With these conventions Porod's formula can be written as follows :

$$\frac{\pi}{2} \underset{s\to\infty}{I_n(s)}\, s^4 = \frac{1}{16\pi^2} \frac{N}{V\bar{\rho}} [(\rho_{par} - \rho_{pol})^2 S_{par} + (\rho_{pol} - \rho_w)^2 S_{pol}] \tag{9}$$

or

$$= \frac{1}{16\pi^2} \frac{N v_{par}}{V\bar{\rho}} \left[(\rho_{par} - \rho_{pol})^2 + (\rho_{pol} - \rho_w)^2 \frac{S_{pol}}{S_{par}} \right] \frac{S_{par}}{v_{par}} \tag{10}$$

where N is the number of particles in the sample.

Having verified that Porod's law does apply, when $\log I_n(s)$ is plotted as a function of logs, the points align along a straight line with slope $n \sim -4$ as shown in figure 9, we can gain access to the geometrical parameters S_{par}/v_{par} and S_{pol}/S_{par} if we know ρ_{par}, ρ_w and ρ_{pol}. In fact, only ρ_{pol} is not known *a priori* ; however it may be determined from the integral of the scattered intensity, which gives access to the mean square value of the fluctuations of the electronic density over the whole sample :

$$4\pi \int_0^\infty s^2 I(s)\, ds = V\overline{(\rho - \bar{\rho})^2} \tag{11}$$

or

$$4\pi \int_0^\infty s^2 I_n(s)\, ds = \frac{1}{\bar{\rho}V} [N v_{par}(\rho_{par}^2 - \rho_w^2) + N v_{pol}(\rho_{pol}^2 - \rho_w^2)] + \frac{\rho_w^2 - \bar{\rho}^2}{\bar{\rho}}. \tag{12}$$

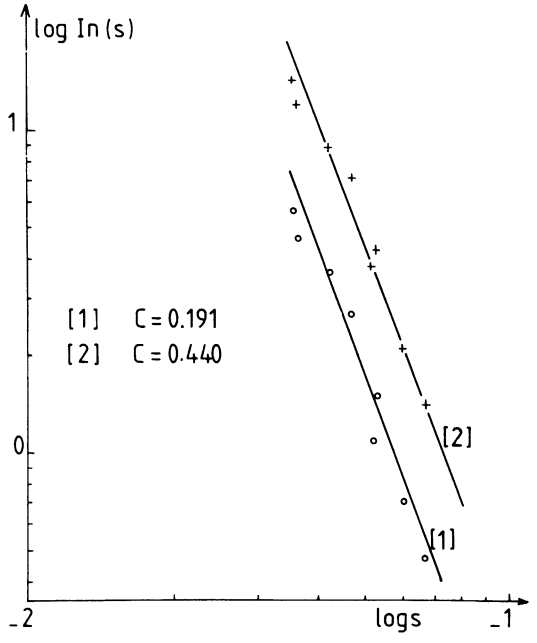

Fig. 9. — Check of Porod's law for two samples. C = amphiphile concentration expressed in grams of solute per gram of solution.

The factor Nv_{par}/V in equations (10) and (12) is easily calculated; v_{par} is replaced by its value calculated from the increment of the electron density of the paraffinic region with respect to water, Δm_{par}, i.e. $v_{par} = \dfrac{\Delta m_{par}}{\rho_{par} - \rho_w}$; it only depends on known parameters characteristic of the sample [22]. The factor Nv_{pol}/V in equation (12) is expressed in an equivalent manner; v_{pol} is replaced by its value calculated from the increment of the electron density of the polar region with respect to water, Δm_{pol}, i.e. $v_{pol} = \dfrac{\Delta m_{pol}}{\rho_{pol} - \rho_w}$; it depends on ρ_{pol} which is not known *a priori*.

One difficulty in calculating the integral (12) is that our knowledge of $I_n(s)$ is limited to

$$1.96 \times 10^{-2}\ \text{Å}^{-1} < s < 6.71 \times 10^{-2}\ \text{Å}^{-1}.$$

The error in the small angle region is negligible, as $s^2 I_n(s)$ is very small at small s. In the large angle region $s^2 I_n(s)$ was estimated according to Porod's law.

The geometrical parameters in equation (10) change with the shape of the aggregates as shown in table I where three types of aggregates are considered for which the general expression

$$\frac{S_{pol}}{S_{par}} = \left(\frac{v_{par} + v_{pol}}{v_{par}}\right)^n$$

is valid. Substituting S_{pol}/S_{par} in equation (10) by its relevant expression, the useful corresponding parameter S_{par}/v_{par} is deduced.

Of course we consider that for each sample the aggregates are monodisperse in shape and size. For the concentrated micellar solutions, close to the nematic phase, this is a quite reasonable assumption considering that the aggregates are rather well defined in the discotic nematic phase [8]. It is also a reasonable assumption for the diluted micellar solutions of long chain amphiphiles as shown in [35].

Table I. — *Expression of the geometrical parameters* S_{pol}/S_{par} *and* S_{par}/v_{par} *as a function of the shape of the aggregate.*

Aggregate	$\dfrac{S_{pol}}{S_{par}} = \left(\dfrac{v_{par} + v_{pol}}{v_{par}}\right)^n$	S_{par}/v_{par}
Sphere	$\left(\dfrac{v_{par} + v_{pol}}{v_{par}}\right)^{2/3}$	$3/R_{par}$
Lamella	$\left(\dfrac{v_{par} + v_{pol}}{v_{par}}\right)^{0}$	$1/R_{par}$ (*)
Cylinder	$\left(\dfrac{v_{par} + v_{pol}}{v_{par}}\right)^{1/2}$	$2/R_{par}$

(*) R_{par} is the thickness of one paraffin layer.

The fitting procedure now consists in calculating S_{par}/v_{par} for each sample and choosing from table I the aggregates whose R_{par} will be closest to the expected relevant length of a C_{10} chain which is ~ 14.3 Å when stretched [36].

The experimental results (the integral of the scattered intensity $4\pi \int_0^\infty s^2 I_n(s)\, ds$ and the Porod's limit, $\lim_{s\to\infty} \frac{\pi}{2} I_n(s)\, s^4$) as well as the calculated parameters (ρ_{pol} and the dimensions R_{par} and R_{pol} related to the shape of the aggregates according the three considered types) are presented in table II for the different values of the amphiphile concentration C, expressed in grams of solute per gram of solution.

5.3.1 $C < 0.191$. — The spherical model is the only one which gives a reasonable R_{par} (R_{par} ~ 12.3 Å). The corresponding aggregate contains 26 molecules and the average area per polar group at the paraffin-polar medium interface is 73 Å^2.

The aggregates of the diluted disordered phases are *isotropic*.

5.3.2 $C > 0.191$. — We can assert the aggregates are not spherical. Indeed if they were spherical the average R_{par} should be ~ 20 Å which is too large when compared to the chain length. Therefore the aggregates of the concentrated disordered phases are to be supposed *anisotropic*. We cannot choose between discotic or calamitic aggregates yet. However owing to the fact that these micellar phases are located in the vicinity of the lyotropic N_d phase, it is tempting to assume that by continuity the aggregates remain discotic.

Table II. — *Experimental data which give access to ρ_{pol} and different parameters related to the shape of the aggregates as a function of the amphiphile concentration C.*

Sample C (g/g)		λ 0.051	χ 0.098	σ 0.191	θ 0.397	η 0.423	ζ 0.440
$I = 4\pi \int_0^\infty s^2 I_n(s)\, ds \times 10^3$		0.79	2.33	3.82	10.82	12.21	13.28
$P = \lim_{s\to\infty} \frac{\pi}{2} I_n(s)\, s^4 \times 10^6$		3.09	9.74	15.77	41.53	43.37	45.81
$I/P \times 10^{-3}$ (*)		0.25	0.24	0.24	0.26	0.28	0.29
ρ_{pol} ($e^-/Å^3$)		0.358	0.406	0.394	0.441	0.425	0.457
R_{sphere} (Å)	R_{par}	7.1	**12.5**	**12.1**	20.1	16.4	24.6
	R_{pol}	11.3	16.3	16.3	24.7	20.6	29.6
$R_{lamella}$ (Å)	R_{par}	2.0	3.5	3.4	5.7	4.7	7.2
	R_{pol}	8.3	7.9	8.3	10.7	9.3	12.5
$R_{cylinder}$ (Å)	R_{par}	4.5	8.0	7.7	12.9	10.4	15.9
	R_{pol}	9.2	11.9	12.0	17.5	14.7	20.9

(*) As outlined in the text, I and P are respectively related to the volume and to the surfaces of discontinuity of the electronic density of the amphiphile. The increase of the ratio I/P in the concentration range near the nematic N_d phase indicates that the shape of the aggregates in the concentrated micellar phases is not the same as in the diluted micellar phases.

Thus the orientation of these isotropic samples under the application of a shear or of a magnetic field discussed above (§ 4.1) correspond to the alignment of anisotropic objects.

6. **Discussion.** — A convenient way to summarize the results of our study is to describe the structural evolution of the samples along the two lines A and B drawn on the phase diagram figure 3. These two lines have been defined on the following ways. A is a line at constant water content (~ 48 %) along which the decanol/SdS ratio increases from 0 to 10.8 %; this line has been chosen in order to show the effect of the alcohol. B is a line at constant SdS/decanol ratio (~ 3.35) along which the water content increases from 40 % to ~ 95 %; it has been chosen in order to determine the effect of diluting the aggregates in water at constant composition of the amphiphile.

6.1 LINE A. — The aggregates contain two amphiphiles, SdS and decanol, and the first is progressively substituted by the other at constant water content. The sequence of the phases is summarized in table III.

The evolution of the structure can be summarized by considering the normal sections of the aggregates and the curvatures of the amphiphile water interfaces. It must be kept in mind that within the investigated domain of the phase diagram (Fig. 3), water is the continuous phase, i.e. the curvature of the amphiphile water interface is convex. Rigorously speaking the symmetry of the normal section decreases, with

Table III. — *Line* A : *Structural evolution at constant water content and increasing decanol content.*

% Decanol (*)	Structure	Aggregates
$0 \leqslant C < 5.0$	H_α Translational order in two dimensions	Infinite cylinders. We assume a circular section (symmetry $\geqslant 6$)
$5.0 < C < 8.5$	R_α^c Translational order in two dimensions	Infinite ribbons with non circular section (symmetry 2)
$10.5 < C < ?$	L_α Translational order in one dimension	Infinite lamellae (symmetry 1)

(*) These approximative values are estimated from the experimental data and the phase diagram sketched in figure 3. So far the exact limits cannot be given as the phase diagram was not been explored on a continuous way.

increasing decanol content, from a value $\geqslant 6$ in the H_α phase to 2 in the R_α^c phase and finally to 1 in the L_α phase. This may be associated, in an intuitive manner, to a decrease of the total curvature of the interface from $1/R$ in the H_α phase with radius R to zero in the L_α phase, across an intermediate value in the R_α^c phase which cannot be estimated in the absence of a determination of the form factor of the aggregates. Also the lateral size of the aggregates increases from 26 Å in the H_α phase to $\sim$ 50 Å in the R_α^c phase, then becomes infinite in the L_α phase.

A clue towards understanding this variation of the curvature under the action of the decanol is provided by studies of mixed monolayers of sodium docosyl sulfate-octadecanol [37] and sodium docosyl sulfate-hexadecanol [38]. Compression isotherms for both systems were recorded with a Langmuir through. It appears that, under constant pressure, the mean area per molecule at the liquid air interface decreases when the molar ratio of alcohol increases. Thus in our system as well, substituting SdS molecules by decanol molecules (which is equivalent to changing the polar heads with keeping the chain length constant), should induce a shrinking of the polar heads in the interfacial layers. The fact that the interface of the H_α phase does not remain circular under this constraint suggests that the layer of paraffinic chains resists the compression. (This has to be paralleled with the conclusion drawn under symmetric conditions : mixtures of potassium soaps whose chain lengths are quite different, one chain about twice as long as the other, studied in the conditions under which the pure soaps are lamellar, have shown that an homogeneous lamellar phase only exist in a very limited concentration range close to the pure lamellar phases. The shorter chains introduce defects of density among the longer ones and as soon as those defects are too numerous the lamellar structure is destroyed. Separation of two lamellar phases occurs but also, in some particular conditions, the amphiphile-water interface bends in order to make the long chains able to fill the defects [39-40]. These two experiments suggest that the conformational state of the chains is rather constant at a given temperature.)

6.2 LINE B. — Aggregates with constant composition in decanol and SdS are diluted. The sequence of the phases is summarized in table IV.

This sequence is characterized by an increase of the interfacial curvature of the aggregates to which is correlated a decrease of the size of the aggregates (they are infinite in the L_α and R_α^c phases, and become finite in the nematic and micellar phases) together with a decrease of their order. This order disappears in several steps : first the translational order is lost at the transition from the R_α^c to the nematic phases, while the orientational order is kept, second this orientational order disappears at the nematic isotropic transition (this is reminiscent of similar sequences observed under the action of the temperature with thermotropic liquid crystals). This evolution of the structures can be qualitatively understood by considering that the water has two effects. At the level of the interface an increase of the degree of hydration favours the repulsive interactions between the polar heads so that the interfacial layer expands [30] but, as discussed above and in [39, 40], the layer of the paraffinic chains resists this expansion; consequently the interface becomes curved and therefore the size of the aggregates must decrease. Also, the rise of water content increases the distances between the aggregates with the effect that their interactions decrease. The disordering of the aggregates results from those two points.

Table IV. — *Line* B : *Structural evolution at constant molar ratio of* SdS/*decanol and increasing water content.*

% Water (*)	Phase	Aggregates
Observed in the range : $C < 47.5$	L_α Translational order in one dimension	Infinite lamellae
$42.0 < C < 52.0$	R_α^c Translational order in two dimensions	Infinite ribbons with non circular section
C around 53.0	N_c Orientational order	Cylinders whose length and section have not been determined yet
C around 54.5	N_d Orientational order	Finite discs
$55.0 < C < 81.0$	Concentrated micellar Isotropic but shear and magnetically induced orientation	Finite anisotropic aggregates, most likely discs
$81.0 \leqslant C < \sim 97.0$	Diluted micellar. Isotropic	Finite isotropic aggregates, spheres

(*) The same remark as below table III is to be made.

7. **Conclusion.** — The existence of nematic phases in a very small region of the phase diagram of SdS-decanol-water system appears to stem out from the rather delicate interplay of the effects of water and decanol. All our experiments were carried out at room temperature and so far the action of the temperature has not been considered. However as already pointed out by L. J. Yu and A. Saupe [27] and observed by us, the nematic phases exist within well defined temperature ranges; in particular when the temperature is raised a N_d nematic phase transform into a N_c nematic phase at a given temperature according to the composition of the mixture. On a similar way when a small amount of salt is added to a N_c nematic phase, it turns out to a N_d nematic phase which aggregates exhibit a lamellar structure [7-8]. An accurate knowledge of

the action of both parameters (temperature, salt) on ordered phases is necessary to make up our description.

The progressive disorganization of the packing of the aggregates as outlined in paragraph 6.2 (the translational order is lost first then the orientational order), reminds of theoretical considerations presenting liquid crystal phases as assemblies of rodlike objects whose organizations are studied as a function of their dimensions and concentration [41-44]. The possibility of calamitic and discotic phases with either uniaxial or biaxial symmetry has been foreseen [43]. The existence of biaxial nematic phases is of special interest [45]. It was recently announced in the system potassium laurate/1-decanol water [46]. In this connection it is of particular interest to consider the location of the N_c phase along the line B ; it appears that it is located in between the translational ordered R_α^c phase, where the aggregates are ribbons with thickness $\sim$ 20 Å and width $\sim$ 50 Å, and the N_d phase, where the aggregates are discs with thickness $\sim$ 20 Å and diameter $\sim$ 60 Å. The close match between the width of the ribbons and the diameter of the discs suggests that the rodlike aggregates of the N_c phase might be also ribbon-like, as in the R_α^c phase. In this case the effect of increasing the water content would be to fragment these ribbons into shorter pieces, this process ultimately leading to the formation of discs in the nematic domain. Thus the aggregates in the nematic phases might have a biaxial symmetry so that biaxial phases might exist. Therefore an important investigation would be that of the evolution of the aggregate sizes at the approach of the phase transitions.

At last when the N_d phase is diluted it becomes isotropic. In the early stage of dilution the aggregates are still anisotropic and we may think they still are disc shaped (although the available evidence does not permit to exclude the existence of finite rod shaped aggregates in this region of the micellar phase). The isotropic phase would therefore result from the loss of orientational order, loss induced by the increase of water content. Then for further dilution the aggregate become isotropic (spherical).

Acknowledgments. — We are indebted to Mrs. A. M. Levelut and Mrs. E. Dartyge for valuable discussions about structural determination and for their technical assistance, to Mr. P. Oswald for his help along the study of the textures and for the photographs of figure 2, to Mr. C. Merienne for his cooperation in the NMR experiments, to Mr. V. Luzzati for fruitful discussions and suggestions, to Mr. B. Cabane for his helpful criticisms on the redaction of the manuscript.

Appendix I. — ESTIMATION OF THE SdS MONOMER CONCENTRATION IN THE MICELLAR SOLUTIONS OF SdS AND DECANOL : MOLAR SdS/DECANOL RATIO $\sim$ 3.35. — The SdS monomer concentration in the micellar solutions of SdS and decanol had to be determined in order to subtract its contribution from the total scattered intensity to obtain that of the micelles. Usually with ionic soluble surfactants the monomer concentration is close to the critical micellar concentration (*CMC*). It is known that small additions of non ionic surfactants, such as long alcohols, lower the *CMC* [47-50] but in our case the molar ratio of decanol/SdS ($\sim 3.35^{-1}$) is high and a precipitation occurs (presumably a gel phase [50]) at a SdS concentration which is much higher than the *CMC*.

For this reason in the presence of rather large amounts of decanol it is only possible to estimate the monomer concentration of SdS. For this purpose we use the NMR method which measures the chemical shifts of the aliphatic protons. As a matter of fact the chemical shifts ν of the proton of the $(CH_2)_\alpha$ groups vary according to the relative population of SdS molecules in and out of the micelles i.e. :

$$\nu = \nu_M + \frac{c_m}{C}(\nu_m - \nu_M)$$

where C is the total SdS concentration, c_m and c_M are the concentrations of monomers and micelles respectively, ν_m and ν_M the chemical shifts when the molecules are either in the monomeric or the micellar state.

When the chemical shifts are plotted as a function of $1/C$ a broken line is observed which corresponds to the existence of two regimes. In the low concentration range, no micelles are present and $\nu(1/C)$ is constant and equal to ν_m, the chemical shift in the monomeric state. In the high concentration range, micelles are present and the SdS molecules exchange between monomeric and micellar states so that $\nu(1/C)$ is no longer constant but varies with the slope $c_m(\nu_m - \nu_M)$. The intersection of both lines yields the inverse of the monomer concentration. According to this method the *CMC* of pure SdS is 3.5×10^{-2} M in agreement with its value given elsewhere [51]. In the case of a SdS-decanol system as the diluted concentration range cannot be attained, therefore the chemical shift of the monomer state measured in the pure SdS systems is used and the monomer concentration is estimated from the intersection of this constant value with the line $\nu(1/C)$ obtained in the micellar range. For the SdS decanol system with molar ratio of decanol SdS $\sim 3.35^{-1}$ the results had a low accuracy owing the precipitation mentioned above, only a small concentration range could be investigated. When the decanol content decreases, the useful concentration range extends and the information becomes more trustworthy. Therefore two other sets of mixed solutions were investigated. For one the molar ratio of decanol/SdS was 5.0^{-1}, for the other 7.8^{-1}. For each system a steep straight line was obtained, the better defined the lower the molar ratio of decanol/SdS is. Its intersection with the asymptotic value $\nu = \nu_m$

relevant to the pure SdS system yields the inverse of the monomer concentration in the solutions. This monomer concentration decreases linearly when the molar ratio of decanol/SdS increases as shown in figure 10. Its value relevant for our experimental conditions (SdS/decanol ~ 3.35) is certainly below 1.8×10^{-2} M.

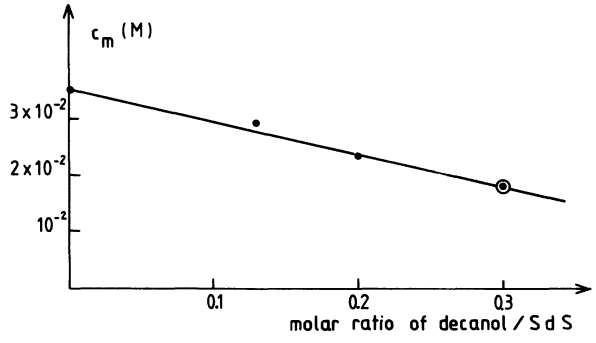

Fig. 10. — SdS monomer concentration, c_m, in SdS-decanol systems as a function of their molar ratio of decanol/SdS. The SdS monomer concentration is estimated using the NMR method which measures the chemical shifts of the aliphatic protons.

Appendix II. — FORM FACTOR AND PACKING OF THE AGGREGATES IN THE R_α^c PHASE. — The angles of the diffraction pattern shown in figure 4*b* give access to the lattice of the R_α^c phase, i.e. to the symmetry and the parameter of the unit cell. The intensities of the reflections may be seen in a general way to depend on the shape and size of the aggregates, and on their orientation in the lattice. To obtain some additional information about the shape and packing of the aggregates, qualitatively appreciated intensities are assigned to the reflection orders as shown in figure 11 where the reciprocal lattice of the R_α^c phase is represented. It appears from the analysis of the relative intensities of the reflections, i.e. from the intensity distribution, the aggregates must be anisotropic in shape. This fact support a ribbonlike shape for the aggregates as suggested. Furthermore the intensity decreases faster along the small dimension in the reciprocal space and suggests the aggregates are packed with their long axis along the large parameter in the real unit cell. This fact is in agreement with our representation of the packing of the aggregates shown in figure 5*b*.

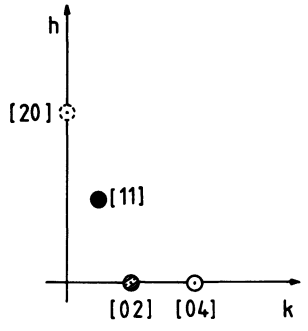

Fig. 11. — The reciprocal lattice of the phase R_α^c (diffraction pattern Fig. 4*b*). The intensities of the reflections (qualitatively estimated) are illustrated [02], ⊘, moderate; [11], ●, strong; [04], ○, weak; [20], ◌, very weak.

References and notes

[1] LAWSON, K. D., and FLAUTT, T. J., *J. Am. Chem. Soc.* **89** (1967) 5489.

[2] The abbreviation SdS is introduced for sodium decyl sulfate instead of SDS in order to avoid confusion with sodium dodecyl sulfate.

[3] ROSEVAER, F. B., *J. Soc. Cosmet. Chem.* **19** (1968) 581.

[4] SAUPE, A., *J. Colloid Interface Sci.* **58** (1977) 549.

[5] RADLEY, K., and SAUPE, A., *Mol. Cryst. Liq. Cryst.* **44** (1978) 227.

[6] BODEN, N., JACKSON, P. H., MCMULLEN, K. and HOLMES, M. C., *Chem. Phys. Lett.* **65** (1979) 476.

[7] CHEN, D. M., FUJIWARA, F. Y. and REEVES, L. W., *Can. J. Chem.* **55** (1977) 2396.

[8] CHARVOLIN, J., SAMULSKI, E. and LEVELUT, A. M., *J. Physique Lett.* **40** (1979) L-587.

[9] BILLARD, J., in *Liquid Crystals of One- and Two-Dimensional Order*, edited by W. Helfrich and G. Hepke (Springer Series in Chemical Physics, Springer Verlag) 1980, p. 383.

[10] SAUPE, A. *et al.* [5] also adopted a structural classification as cylindrical and lamellar nematics. We propose the terms calamitic and discotic as a less constraining representation of the shapes of the aggregates. Also it is not certain at the moment that the structural and magnetic classifications are equivalent, for instance with SdS the type II is N_d but with caesium perfluorooctanoate N_d might be of type I. See BODEN, N., MCMULLER, K. J., HOMMES, M. C. and TIDDY, G. J. T., in *Liquid Crystals of One- and Two-Dimensional Order*, edited by W. Helfrich and G. Hepke (Springer Verlag) 1980, p. 299.

[11] EKWALL, P., in *Liq. Cryst.* **1** (Acad. Press) 1975. No « nematic » domain is apparent in the phase diagrams of the systems Na octyl sulfate-decanol-water and Na dodecyl sulfate decanol-water shown by P. Ekwall (Fig. 64 and Fig. 65).

[12] LUZZATI, V., MUSTACCHI, H., and SKOULIOS, A., *Disc. Faraday Soc.* **25** (1958) 43.

[13] LUZZATI, V., MUSTACCHI, H., SKOULIOS, A. et HUSSON, F., *Acta Crystallogr.* **13** (1960) 660.

[14] HUSSON, F., MUSTACCHI, H. et LUZZATI, V., *Acta Crystallogr.* **13** (1960) 668.

[15] SKOULIOS, A. et LUZZATI, V., *Acta Crystallogr.* **14** (1961) 278.

[16] SKOULIOS, A., *Adv. Colloid Interface Sci.* **1** (1967) 79.

[17] CHARVOLIN, J. and TARDIEU, A., *Lyotropic liquid Crystals, Structures and molecular Motions* in Solid State Physics Suppl. **14**, edited by F. Seitz and D. Turnbull (Acad. Press) 1978.

[18] STRZELECKI, L. and GERMAIN, C., according the synthesis : RADLEY, K., REEVES, L. W. and TRACEY, A. S., *J. Phys. Chem.* **80** (1976) 174.

[19] KURZ, J. L., *J. Phys. Chem.* **66** (1962) 2239.
[20] GUINIER, A., *Théorie et Technique de Radiocristallographie* (Dunod, Paris).
[21] LUZZATI, V., *Acta Crystallogr.* **13** (1960) 939.
[22] REISS-HUSSON, F., Thèse d'Etat, Faculté de l'Université de Strasbourg (1963).
[23] REISS-HUSSON, F. and LUZZATTI, V., *J. Colloid Interface Sci.* **21** (1966) 534.
[24] LEVELUT, A. M., LAMBERT, M. et GUINIER, A., *C.R. Hebd. Séan. Acad. Sci.* **255** (1962) 319.
DARTYGE, E., Thèse d'Etat, Faculté des Sciences d'Orsay, Université Paris-Sud (1979).
[25] LEVELUT, A. M. et GUINIER, A., *Bull. Soc. Fr. Minéral. Cristallogr.* **XC** (1967) 445.
[26] LACHAMPT, F. et VILLA, R. M., *Revue Française des Corps Gras* n° **2** (1969) 87.
[27] YU, L. J. and SAUPE, A., *J. Am. Chem. Soc.* **102** (1980) 4879.
[28] KLEMAN, M., *J. Physique* **41** (1980) 737.
[29] KLEMAN, M. and OSWALD, P., private communication.
[30] LUZZATTI, V., in *Biological Membranes*, edited by D. Chapman, (Academic Press) 1968, p. 71.
[31] CHARVOLIN, J. and HENDRIKX, Y. in *Liquid Crystals of One- and Two-Dimensional Order*, edited by W. Helfrich and G. Hepke (Springer Series in Chemical Physics, Springer Verlag) 1980, p. 265.
[32] AMARAL, L. Q., PIMENTEL, C. A., TAVARES, M. R. and VANIN, J. A., *J. Chem. Phys.* **71** (1979) 2980.
[33] HENDRIKX, Y., CHARVOLIN, J., RAWISO, M. and LIEBERT, L., in preparation.
[34] GUINIER, A. and FOURNET, G., *Small-Angles Scattering of X-rays* (John Wiley and Sons, Inc., New York) 1955.
[35] RHODE, A. and SACKMANN, E., *J. Colloid Interface Sci.* **70** (1979) 494.
[36] TANFORD, C., *Hydrophobic Effect* (Wiley, Interscience Publication, N. Y.) 1973.
[37] COSTIN, J. S. and BARNES, G. J., *J. Colloid Interface Sci.* **51** (1975) 94.
[38] HENDRIKX, Y. et MARI, D., *Physico-chimie des composés Amphiphiles* (éditions du Centre National de la Recherche Scientifique, Paris) 1979.
[39] MELY, B. et CHARVOLIN, J., *Physico-chimie des composés amphiphiles* (éditions du Centre National de la Recherche Scientifique, Paris) 1979.
[40] CHARVOLIN, J. and MELY, B., *Mol. Cryst. Liq. Cryst. Lett.* **41** (1978) 209.
[41] ONSAGER, L., *Phys. Rev.* **62** (1942) 558.
[42] ISIHARA, A., *J. Chem. Phys.* **19** (1951) 1142.
[43] SHIH, C. and ALBEN, R., *J. Chem. Phys.* **57** (1972) 3055.
[44] DEBLIEK, R. and LEKKERKERKER, H. N. W., *Liquid Crystals of One- and Two-Dimensional Order*, edited by W. Helfrich and G. Hepke (Springer Series in Chemical Physics, Springer Verlag) 1980, p. 289.
[45] TOULOUSE, G., *J. Physique Lett.* **38** (1977) L-67.
[46] YU, L. J. and SAUPE, A., *Phys. Rev. Lett.* **45** (1980) 1000.
[47] SHINODA, K., *J. Phys. Chem.* **58** (1954) 1136.
[48] SCHICK, M. J. and FOWKES, F. M., *J. Phys. Chem.* **61** (1957) 1062.
[49] SHIRAMA, K. and KASHIWABARA, T., *J. Colloid Interface Sci.* **36** (1971) 65.
[50] NAKAYAMA, H., SHINODA, K. and HUTCHINSON, E., *J. Phys. Chem.* **70** (1966) 3502.
[51] MUKERJEE, P. and MYSELS, K. J., *Critical Micelle Concentrations of aqueous Surfactant Systems*, NSDR-NBS 36 (1971).